Growth patterns of non-enhancing glioma assessed on DTI-derived isotropic and anisotropic maps are not associated with IDH mutation or 1p19q codeletion status

Renske Gahrmann
Jochem Spoor
Maarten Wijnenga
Sieger Leenstra
Arnaud Vincent
Marius de Groot
Pim French
Martin van den Bent
Marion Smits

SUBMITTED

ABSTRACT

Background. Extent of mismatch between tumor delineations drawn on Diffusion Tensor Imaging (DTI) derived isotropic (*p*) and anisotropic (*q*) maps have been shown to distinguish isocitrate dehydrogenase (*IDH*) *wild-type* (*wt*) and *mutated* (*mt*) glioblastomas. We use this technique in non-enhancing gliomas to determine if an assessment of *IDH*-mutation as well as 1p19q codeletion status can be made.

Methods. All patients undergoing presurgical DTI for non-enhancing glioma between 2004 and 2013 from a single center were included (n=83). A targeted Next-Generation Sequencing panel (NGS) was used to determine the presence of *IDHmt* and 1p19q codeletion. A volume of interest (VOI) was drawn on the *p*-map and subsequently overlaid on the *q*-map to determine overlap with white matter tracts (>0.5cm) by 2 observers. Extent and pattern of mismatch was scored as: I) no indication of infiltration (i.e. no *p/q* mismatch), II) single focus of infiltration, III) multifocal infiltration, IV) expansion of lesion into white matter tracts, and V) infiltration following white matter tracts. Different patterns found in *IDHmt* versus *IDHwt* and 1p19q codeleted versus non-codeleted tumors were compared with a Mann-Whitney U test. Cohen's Kappa was calculated to assess interobserver agreement.

Results. Four of the non-enhancing gliomas were *IDHwt*, 29 were both *IDHmt* and 1p19q codeleted, and 50 *IDHmt* without 1p19q codeletion. The 4 *IDHwt* gliomas all had a different pattern of infiltrative growth (i.e. patterns II, III, IV, and V). These same patterns were also seen in the *IDHmt* glioma group. No significant differences between codeleted and non-codeleted tumors were found (Mann-Whitney U=714.0, p=.908). The interobserver agreement was moderate with a Kappa of 0.473 (SE=0.068) or 62.7%.

Conclusion. Because of overlap in growth patterns between *IDHwt* versus *IDHmt* and 1p19q codeleted versus non-codeleted gliomas and the suboptimal interobserver concordance, this DTI-derived technique does not allow for the distinction of possible different molecular subtypes in non-enhancing gliomas.

Advances in knowledge

- Patterns of mismatch between DTI-derived isotropic and anisotropic maps do not predict *IDH*-mutation or 1p19q codeletion status in non-enhancing gliomas.
- While successfully applied in glioblastoma, this technique has moderate inter-rater agreement when used for assessment of non-enhancing glioma growth patterns.

Implications for patient care

- Possible differences in growth pattern between non-enhancing glioma molecular subtypes could not be distinguished using *p/q* mapping and so we currently do not recommend using this technique for non-enhancing gliomas in a clinical setting.

Summary statement

Previous research indicates that different molecular subtypes of glioblastoma (i.e. *IDH*-mutated versus *IDH* wild-type) can be discerned based on the extent/pattern of mismatch assessed on isotropic and anisotropic diffusion maps. Using this same technique in non-enhancing glioma, we found no differences in growth pattern between *IDH*-mutated versus *IDH* wild-type and 1p19q codeleted versus non-codeleted tumors.

INTRODUCTION

The 2016 update of the WHO classification for central nervous system tumors presents a major change in the classification of gliomas: not only histological, but also molecular features now characterize different types of gliomas. The WHO 2016 classification distinguishes between two types of astrocytoma based on the mutational status of the gene encoding for isocitrate dehydrogenase (*IDH*) 1 or 2: *IDH*-mutant (*IDHmt*) and *IDH* wild-type (*IDHwt*) astrocytoma. Oligodendroglioma are characterized by the presence of a codeletion of chromosomal arms 1p and 19q and an *IDH1/2* mutation[1]. The incidence of *IDH* mutation in grade II and III gliomas (according to the WHO 2007 classification) is 60-80%, leaving a subset of lower-grade glioma to be *IDHwt*[2]. Many of these *IDHwt* tumors with grade II or III histological features present without enhancement on imaging. The prognosis of these patients is poor compared to that of patients with *IDHmt* gliomas especially in the presence of a TERT promotor mutation[3].

IDHmt gliomas with a 1p19q codeletion (oligodendrogliomas) have a better prognosis than those without a codeletion (astrocytoma, *IDHmt*). A non-invasive identification of the different molecular subtypes of non-enhancing gliomas can help discern a subgroup of more aggressive tumors from the more indolent ones. Not only will this lead to a more accurate prediction of molecular subtypes, but it may also aid in guiding treatment decisions.

The presence of enhancement is generally considered a sign of aggressiveness, however in its absence, other characteristics, such as growth patterns could be informative. Differences in glioma growth between subtypes of non-enhancing tumors (oligodendroglioma and *IDHmt* or *IDHwt* astrocytoma) have not been extensively explored. Infiltrative growth has been reported in both astrocytoma and oligodendroglioma, although in oligodendrogliomas areas with more compact infiltration can also be present[4]. Glioma infiltration occurs along perineuronal structures (also known as perineuronal satellitosis), subpial, and perivascular structures, as well as along white matter fibers. In extreme cases, the tumor infiltrates throughout the brain resulting in a gliomatosis cerebri pattern seen on imaging[5].

While displacement or destruction of white matter tracts is fairly easy to determine, infiltration of a tract is more difficult to assess[6]. With Diffusion Tensor Imaging (DTI) the microstructural properties of different tissues can be determined by measuring diffusion of water molecules. When water molecules are restricted in their diffusion, such as in the presence of white matter tracts, this is reflected in DTI-derived parameters of anisotropy (q) and isotropy (p)[7]. The use of q eliminates the possible confounding effect of changes in the overall diffusion, as is the case when measuring the fractional anisotropy (FA). Combining anisotropic measures with isotropic

measures, such as Mean Diffusivity (MD), Apparent Diffusion Coefficient (ADC), and pure isotropy (*p*) can help determine tumor infiltration along white matter tracts. In enhancing/high-grade tumor it has been shown that in biopsy-proven areas of infiltration, *p* is abnormally high, while *q* is within a normal range[8-10]. The mismatch between *p* and *q* has been used by Price et al. to determine the extent of infiltrative growth along white matter tracts in *IDHmt* and *IDHwt* glioblastoma[11,12]. In IDHmt (and 8% of *IDHwt*) glioblastoma, a minimally invasive pattern was found, while in IDHwt glioblastoma, a locally invasive or diffusely invasive pattern was encountered[10]. These findings led us to apply this technique in the group of patients with presumed low-grade gliomas (i.e. non-enhancing tumors without necrosis).

We hypothesize that assessing the 'mismatch' between *p* and *q* could help visualize different growth patterns in non-enhancing gliomas and as such differentiate non-invasively between the molecularly defined glioma subtypes similar to previous findings in glioblastoma.

METHODS

Patients

Adult patients with suspected low-grade glioma (i.e. without enhancement and necrosis) that had undergone presurgical functional MRI (fMRI) and DTI between December 2004 and June 2014 in the Erasmus MC in Rotterdam (NL) were considered for retrospective analysis. Approximately 125 patients with suspected low-grade glioma were operated in this timeframe, 90 of whom had undergone presurgical DTI in preparation of awake-surgery. Targeted Next-Generation Sequencing panel (NGS) was performed on the archival tumor tissue to determine presence of *IDH1*- and *IDH2*-mutations and 1p19q codeletion and other molecular lesions characteristic of glioblastoma[13]. The institutional review board approved of the design of the study. Previously, Wijnenga et al.[3] reported on 65 of the 90 patients included in our study focusing on pre- and postoperative tumor volumes in relation to molecular information; DTI-data was not included in this prior analysis.

Tumors were categorized according to the presence or absence of an *IDH*-mutation (*IDHmt* respectively *IDHwt*) and 1p19q codeletion according to the WHO 2016 classification[1]. Patients with partial imbalance or loss of only one chromosomal arm were categorized as non-codeleted. Overall Survival (OS) was defined in years from the date of the preoperative DTI-scan until death.

Data acquisition and processing

All scanning was performed at 1.5 or 3.0 tesla field strength (GE Healthcare, Milwaukee, IL, USA) with a matrix of 256x256 and an in-plane resolution of less than 1mm^2. All data were acquired with a minimum of 25 directions (all with b=1000 s/mm^2) and 1-4 b=0 s/mm^2 images. For more details see ***Supplementary Files table S1***.

DICOM files were converted to NIfTI format for processing in FSL (Oxford, UK)[14]. Images were reoriented and corrected for eddy currents using the b=0 s/mm^2 image as a reference. The brain was extracted using BET (Brain Extraction Tool)[15] with a threshold of 0.3. FSL-DTIFit was used to extract the eigenvectors, eigenvalues and mean diffusivity, which were then used to create a pure isotropic map (*p*) and an anisotropic map (*q*) with a custom script using FSLmaths according to equations from Price et al.[16]:

$$p = \sqrt{3D}$$

$$q = \sqrt{(\lambda_1 - D)^2 + (\lambda_2 - D)^2 + (\lambda_3 - D)^2}$$

Where *D* is the mean diffusivity and λ the eigenvalues:

$$D = (\lambda_1 + \lambda_2 + \lambda_3)/3$$

Data analysis

A volume of interest (VOI) of the tumor area was drawn manually by one observer on the *p*-map using MRIcron (Chris Rorden, www.mricro.com, version 6.6.2013). Clearly recognizable blood vessels were excluded.

We overlaid the VOI from the *p*-map on the *q*-map to visually determine overlap with white matter tracts (i.e. high-intensity areas on the *q*-map). A VOI exceeding >0.5cm in three directions over such high intensity areas was considered to be a *p/q*-mismatch, indicating infiltration of the white matter tract[8] (***Figure 1***). The *p/q* mismatch was categorized by two independent observers (i.e. an experienced neuroradiologist and a radiology resident) as follows: I) no indication of infiltration (i.e. no *p/q* mismatch), II) single focus of infiltration, III) multifocal infiltration, IV) expansion of lesion into white matter tracts, and V) infiltration following white matter tracts (***Figure 2***). A combination of options was allowed. Both observers were blinded for histological and molecular tumor status. Interobserver agreement was determined by calculating Cohen's Kappa Coefficient. In case of discrepancy, the maps were reviewed again by the two observers together to assign the category in consensus, which was then used for further analyses. The difference in incidence within each *p/q* mismatch category between molecular tumor categories was compared using a Mann-Whitney U test.

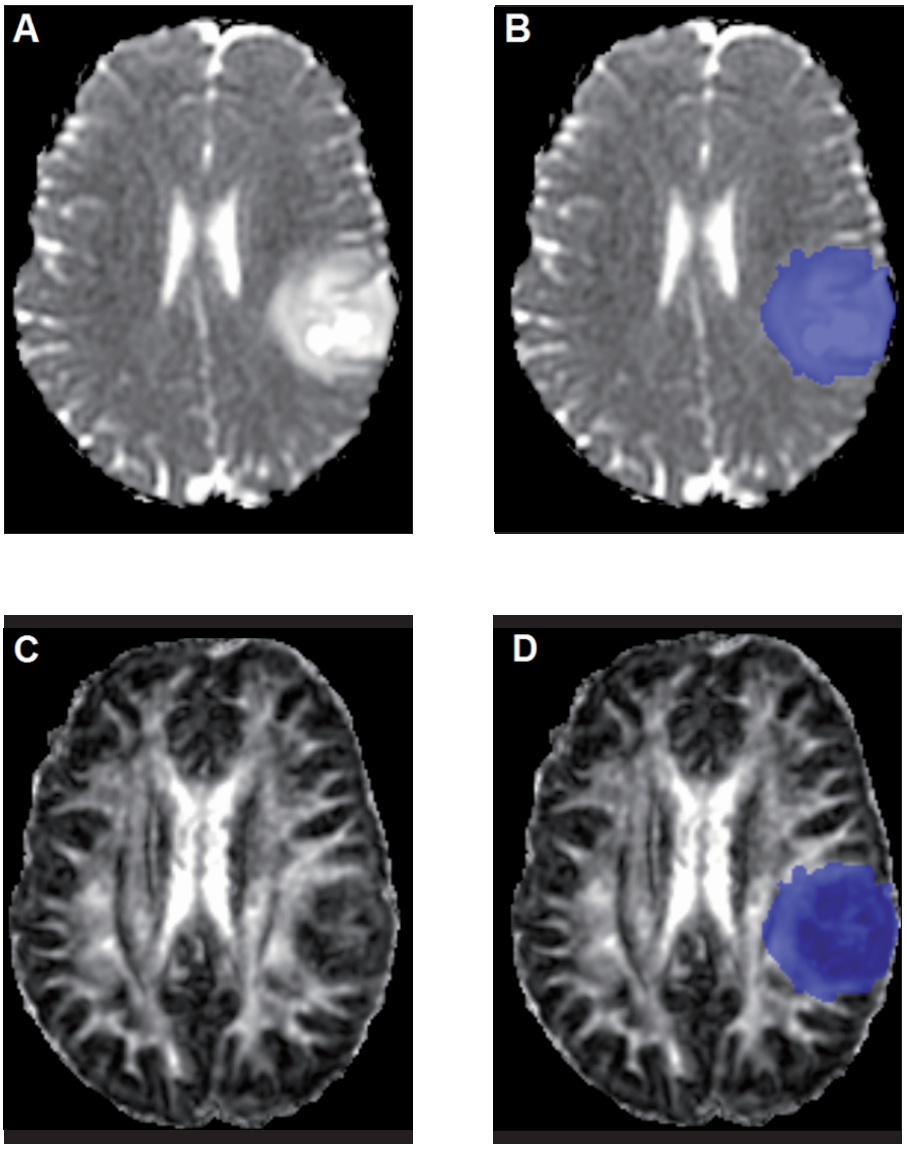

Figure 1. Example of a non-enhancing tumor with a peripheral localization, clearly visible on the *p*-map (**A**). Tumor segmentation was performed on the *p*-map (**B**) and subsequently overlaid on the *q*-map (**C**, **D**). An additional line drawn on image **D** shows the location of mismatch. This example was classified as 'expansion of lesion into white matter tracts'.

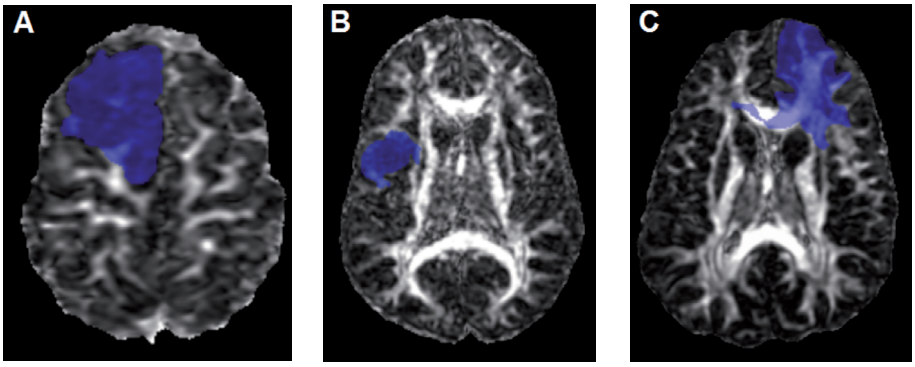

Figure 2. Examples of different *p/q* mismatch patterns: 'single focus of infiltration' (**A**), 'multifocal infiltration' (**B**), and 'infiltration following white matter tracts' (**C**). Additional lines have been drawn to show the location of mismatch.

RESULTS

Patients

In 7 patients NGS could not be performed since there was no tumor tissue available. The final analysis was performed on the remaining 83 patients (49 men and 34 women). Mean and median age was 39 years (range, 20 to 72 years). At the time of analysis, 29 patients had died with a median OS of 4.2 years (range, 0.9 to 9.2 years). Four (13.8%) of these patients had a 1p19q codeleted tumor.

Tumors were located in the frontal lobe in 41 (49.4%), the insula in 17 (20.5%), temporal lobe in 9 (10.8%), and parietal lobe in 4 (4.8%) patients. The remaining tumors were located in both the frontal and parietal lobes in 5 (6.0%), the parietal and temporal lobes in 5 (6.0%), and in more than 2 lobes in 2 (2.4%) patients. There was a left hemispheric predominance, with 69.9% (n=58) of tumors located in the left hemisphere.

Molecular data

In 79 of 83 patients, an *IDH1* or *IDH2* mutation was found with the main subtype *IDH-R132H* found in 66 patients. Other subtypes found were *R132C* (n=4), R132G (n=3), *IDH1-R132S* (n=2), *IDH2-R172K* (n=3), and *IDH2-R172M* (n=1). Four patients with an *IDHwt* tumor were deceased at the time of analysis with a median OS of 2.0 years (range, 2.5 to 4.2 years). In the *IDHmt* tumor group, 25 (31.6%) patients had died with a median OS of 4.4 years (range, 0.9 to 9.2 years). Additional molecular information in the 4 *IDHwt* patients revealed TERT mutations (all 4), imbalance or loss of chromosome 7 and 10 (including PTEN; 3 patients), and EGFR amplification (2 patients), all corresponding with glioblastoma[13].

In the 79 *IDHmt* tumors, 29 (34.9%) were 1p19q codeleted, while 50 tumors were non-codeleted. The 2 tumors growing in more than 2 lobes were both *IDHmt* without a 1p19q codeletion.

p/q assessment

A discrepancy between the initial ratings by the 2 observers was present in 31 (37.3%) cases. In the discrepant cases, consensus was reached by agreeing with observer 1 in 11 cases and with observer 2 in 14 cases. In the remaining 6 cases a new category was assigned. All final ratings are shown in ***Table 1***. The interobserver agreement was moderate with Kappa=0.473 (SE=0.068).

Table 1. Incidence of *p/q* mismatch categories (final assessment by 2 observers in consensus) in molecularly defined glioma subtypes. WM=white matter.

p/q mismatch category	IDHmt (n=79)	IDHwt (n=4)	1p19q codeleted (n=29)	1p19q non-codeleted (n=50)
I No indication of infiltration	2 (2.5%)		-	2 (4%)
II Single focus of infiltration	4 (5.1%)	1 (25%)	1 (3.4%)	3 (6%)
III Multifocal infiltration	23 (29.1%)	1 (25%)	10 (34.5%)	13 (26%)
IV Expansion of lesion into WM tracts	25 (31.6%)	1 (25%)	9 (31%)	16 (32%)
V Infiltration following WM tracts	20 (25.3%)	1 (25%)	7 (24.1%)	13 (26%)
III and **IV**	3 (3.8%)	-	-	3 (6%)
IV and **V**	2 (2.5%)	-	2 (6.9%)	-

The predominant *p/q* mismatch categories in the *IDHmt* group were III) multifocal infiltration (29.1%), IV) expansion of lesion into white matter tracts (31.6%), and V) infiltration following white matter tracts (25.3%). The 4 patients with *IDHwt* tumor each showed a different category of *p/q* mismatch, i.e. II) single focus of infiltration, III) multifocal infiltration, IV) expansion of lesion into white matter tracts, and V) infiltration following white matter tracts, rendering these 4 *IDHwt* tumors indistinguishable from the *IDHmt* tumors.

In the 1p19q codeleted group (n=29) and non-codeleted group (n=50), the main *p/q* mismatch categories were III (34.5% respectively 26.0%), IV (31.0% respectively 32.0%), and V (24.1% respectively 26.0%). No significant difference in the incidence of *p/q* mismatch categories was found between these two groups: Mann-Whitney U=714.0, p=.91.

DISCUSSION

Our study showed that the major groups of molecularly defined glioma subtypes (oligodendroglioma and *IDHmt* or *IDHwt* astrocytoma) in non-enhancing gliomas cannot be discerned based on infiltrative growth pattern assessed on DTI-derived isotropic and anisotropic maps. The 4 *IDHwt* tumors each showed a different pattern of tumor growth, while no differences in the various growth patterns between 1p19q codeleted and non-codeleted tumors were observed.

Glioma growth can lead to destruction, infiltration, edema or displacement of white matter tracts[6,17]. Destruction and tract displacement are easily recognized. A displaced tract can still be intact despite being compressed (sometimes increasing anisotropic values)[18]. Infiltration and edema of white matter tracts are more difficult to assess, as in both we see an increase in isotropic and a variable decrease in anisotropic values. In infiltrated white matter tracts the anisotropy is dependent on the amount of tumor infiltration and the degree to which the tracts are intact[18]. Different models looking at glioma growth find that anisotropic parameters are more suited to assess tumor infiltration than isotropic parameters[19-22].

Anisotropic values (*q* or FA), however, need to be looked at in context with isotropic values (*p* or MD or ADC). In the gross tumor, *p* or MD is increased and *q* or FA is reduced compared to normal tissue. But regions surrounding the tumor (high T2w signal) can consist of edema and/or infiltrating tumor, leading to abnormally high *p* or MD values, while *q* or FA values may be within normal range[8,9,23]. This mismatch between *p* and *q* has successfully been used to describe different infiltrative patterns in *IDHmt* and *IDHwt* glioblastoma by Price et al. They describe three different patterns of infiltration: a minimally invasive pattern, which is seen in all *IDHmt* and in 8% of *IDHwt* glioblastomas, a locally invasive pattern, and a diffusely invasive pattern seen in 23% and 69% of *IDHwt* glioblastomas respectively[10-12]. We used a slightly adapted categorization of these mismatch patterns to better capture the different growth patterns we encountered in non-enhancing gliomas. Categories I and II ('no indication of infiltration' and 'single focus of infiltration') are similar to Price et al.'s 'minimally invasive' pattern. In patients with more extensive white matter tract infiltration, however, we found both tumors that clearly followed white matter tracts and tumors that expanded into a large section of the tract. This distinction was felt not to be captured by simply categorizing both growth patterns as 'diffusely invasive', and thus further specified in our categorization.

Based on Price et al.'s findings in glioblastoma, we expected the non-enhancing *IDHwt* tumors (even if only present in 4 patients) to predominantly expand into or to infiltrate along white matter tracts and *IDHmt* tumors to express a less invasive growth pattern. Instead, we found that each of the 4 *IDHwt* tumors had a different

pattern of growth, ranging from minimally invasive (single focus of infiltration) to infiltration along white matter tracts. These same patterns were found in the *IDHmt* group. We were therefore unable to identify the *IDHwt* tumors based on their growth patterns as assessed with *p/q* mapping. Similarly, we were unable to distinguish 1p19q codeleted from non-codeleted tumors with this technique. Possible explanations for the lack of 'positive' findings are first that growth patterns between these molecular subtypes are in fact not significantly different, and second that potentially existing differences cannot be distinguished with *p/q* mapping.

Very little is known about growth patterns of non-enhancing glioma molecularly defined subtypes. Both codeleted (oligodendroglioma) and non-codeleted (astrocytoma) gliomas are known to infiltrate along white matter tracts, but this seems to be more common in astrocytoma[24,25]. It should be noted that these previous studies included both enhancing and non-enhancing tumors. While based on these studies on 1p19q codeletion and the study by Price et al. on *IDH*-mutation status in glioblastoma[10] differences in growth pattern between molecularly defined glioma subtypes are conceivable, it is possible that these findings can not be translated to the non-enhancing, lower grade (II/III) tumors and that in these tumors no significant differences in growth pattern are in fact present.

Alternatively, our 'negative' results may be related to the *p/q* mapping technique. We found that determining growth patterns in small and peripherally located tumors was problematic: in the peripheral, smaller tracts, the threshold for *p/q* mismatch of 0.5cm[10] was difficult to apply, because the lower anisotropy in the peripheral tracts hindered assessment of further reduction in anisotropy due to tumor infiltration. This likely contributed to the low agreement between the observers (62.7%). Price et al. reported an interobserver agreement of 90% (26), a difference that can be explained the study population (glioblastoma versus non-enhancing glioma) as well as the different number of categories (3 versus 5 categories).

The retrospective nature of this study introduced a selection bias towards patients who were eligible for awake-surgery, because preoperative DTI is only performed for these surgeries at our institution. These patients are generally in a better condition and of a younger age than those not selected for awake surgery and more often have a tumor located in the left hemisphere (for preservation of language function). This selection bias may also have resulted in the low number of only 4 *IDHwt* gliomas, since patients with *IDHwt* tumors tend to be older and thus less eligible for awake surgery. We furthermore only included non-enhancing gliomas, in which *IDHwt* is likely to be less frequent than in enhancing tumors. Despite this low number, it was clear that each of the *IDHwt* gliomas showed a different growth pattern that overlapped with patterns seen in *IDHmt* tumors. Our conclusion that *p/q* mapping in these patients does not distinguish between *IDHwt* and *IDHmt* thus remains valid.

In conclusion, we were unable to translate previous findings from glioblastoma, showing that *p/q* mapping can be used to discern different molecular subtypes, to non-enhancing glioma. Based on our findings, we do not recommend using this technique to determine molecular status in non-enhancing glioma.

REFERENCES

1. Louis DN, Perry A, Reifenberger G, et al. The 2016 World Health Organization classification of tumors of the central nervous system: a summary. Acta Neuropathol 2016;131(6):803-820.
2. Hartmann C, Meyer J, Balss J, et al. Type and frequency of IDH1 and IDH2 mutations are related to astrocytic and oligodendroglial differentiation and age: a study of 1,010 diffuse gliomas. Acta Neuropathol 2009;118(4):469-474.
3. Wijnenga MMJ, French PJ, Dubbink HJ, et al. The impact of surgery in molecularly defined low-grade glioma: an integrated clinical, radiological and molecular analysis. Neuro Oncol 2017 sep 7 (Epub ahead of print).
4. Capper D, Weissert S, Balss J, et al. Characterization of R132H mutation-specific IDH1 antibody binding in brain tumors. Brain Pathol 2010;20(1):245-254.
5. Claes A, Idema AJ, and Wesseling P. Diffuse glioma growth: a guerilla war. Acta Neuropathol 2007; 114(5):443-458.
6. Yen PS, Teo BT, Chiu CH, Chen SC, Chiu TL, Su CF. White matter tract involvement in brain tumors: a diffusion tensor imaging analysis. Surg Neurol 2009;72(5):464-469.
7. Jones DK, Leemans A. Diffusion tensor imaging. Methods Mol Biol 2011;711:127-144.
8. Price SJ, Jena R, Burnet NG, et al. Improved delineation of glioma margins and regions of infiltration with the use of diffusion tensor imaging: an image-guided biopsy study. AJNR Am J Neuroradiol 2006;27(9):1969-1974.
9. Pena A, Green HA, Carpenter TA, Price SJ, Pickard JD, Gillard JH. Enhanced visualization and quantification of magnetic resonance diffusion tensor imaging using the p:q tensor decomposition. Br J Radiol 2006;79(938):101-109.
10. Price SJ, Jena R, Burnet NG, Carpenter TA, Pickard JD, Gillard JH. Predicting patterns of glioma recurrence using diffusion tensor imaging. Eur Radiol 2007;17(7):1675-1684.
11. Price SJ, Allinson K, Liu H, et al. Less invasive phenotype found in isocitrate dehydrogenase-mutated glioblastomas than in isocitrate dehydrogenase wild-type glioblastomas: a diffusion-tensor imaging study. Radiology 2017;283(1):215-221.
12. Mohsen LA, Shi V, Jena R, Gillard JH, Price SJ. Diffusion tensor invasive phenotypes can predict progression-free survival in glioblastomas. Br J Neurosurg 2013;27(4):436-441.
13. Dubbink HJ, Atmodimedjo PN, Kros JM, et al. Molecular classification of anaplastic oligodendroglioma using next-generation sequencing: a report of the prospective randomized EORTC Brain Tumor Group 26951 phase III trial. Neuro Oncol 2016;18(3):388-400.
14. Jenkinson M, Beckmann CF, Behrens TE, Woolrich MW, Smith SM. FSL. Neuroimage 2012;62(2): 782-790.
15. Smith SM. Fast robust automated brain extraction. Hum Brain Map 2002;17(3):143-155.
16. Price SJ, Pena A, Burnet NG, et al. Tissue signature characterization of diffusion tensor abnormalities in cerebral gliomas. Eur Radiol 2004;14(10):1909-1917.
17. Price SJ, Gillard JH. Imaging biomarkers of brain tumour margin and tumour invasion. Br J Radiol 2011;84 Spec No 2:S159-167.
18. Goebell E, Paustenbach S, Vaeterlein O, et al. Low-grade and anaplastic gliomas: differences in architecture evaluated with diffusion-tensor MR imaging. Radiology 2006;239(1):217-222.
19. Jbabdi S, Mandonnet E, Duffau H, et al. Simulation of anisotropic growth of low-grade gliomas using diffusion tensor imaging. Magn Reson Med 2005;54(3):616-624.
20. Painter KJ, Hillen T. Mathematical modeling of glioma growth: the use of Diffusion Tensor Imaging (DTI) data to predict the anisotropic pathways of cancer invasion. J Theor Biol 2013;323:25-39.

21. Schlüter M, Stieltjes B, Hahn HK, Rexillius J, Konrad-verse O, Peitgen HO. Detection of tumour infiltration in axonal fibre bundles using diffusion tensor imaging. Int J Med Robot 2005;1(3):80-86.

22. Stadlbauer A, Ganslandt O, Buslei R, et al. Gliomas: histopathological evaluation of changes in directionality and magnitude of water diffusion at diffusion tensor MR imaging. Radiology 2006; 240(3):803-810.

23. Wright AJ, Fellows G, Byrnes TJ, et al. Pattern recognition of MRSI data shows regions of glioma growth that agree with DTI markers of brain tumor infiltration. Magn Reson Med 2009;62(6):1646-1651.

24. Jenkinson MD, du Plessis DG, Smith TS, Joyce KA, Wamke PC, Walker C. Histological growth patterns and genotype in oligodendroglial tumours: correlation with MRI features. Brain 2006;129(Pt 7):1884-1891.

25. Chen S, Tanaka S, Giannini C, et al. Gliomatosis cerebri: clinical characteristics, management, and outcomes. J Neurooncol 2013;112(2):267-275.

26. Price SJ, Young AM, Scotton WJ, et al. Multimodal MRI can identify perfusion and metabolic changes in the invasive margin of glioblastomas. J Magn Reson Imaging 2016;43(2):487-494.

SUPPLEMENTARY FILES

Table S1. number of patients scanned per type of scanner and corresponding settings, including the number of B=0 s/mm^2 and B=1000 s/mm^2 images (diffusion directions) scanned.

Scanner (GE)	Number of patients	TR (ms)	TE (ms)	b=0/b=1000 (s/mm^2)	Slice thickness (mm)	Matrix	Pixel size (mm)
SIGNA EXCITE (3 tesla)	44	14200**	70-85	1-3/25	2.0	256x256	0.859
DISCOVERY MR450 (1.5 tesla)	21	8000	81-85	1-3/25	2.0 5.0*	256x256	0.977
SIGNA EXCITE (1.5 tesla)	13	8000	68-73	1-3/25	3.5	256x256	0.820
Signa HDxt (3 tesla)	4	16000	86	4/31	2.0	256x256	0.820
DISCOVERY MR750 (3 tesla)	1	7925	88	4/32	2.5	256x256	0.938

* 5 patients were scanned with 5mm slice thickness.

** 4 deviations from protocol with TRs of 16000, 15525, 15450 and 15500